

RESEARCH PAPER

Hydraulic efficiency and coordination with xylem resistance to cavitation, leaf function, and growth performance among eight unrelated *Populus deltoides* × *Populus nigra* hybrids

Régis Fichot^{1,2,3,*}, Sylvain Chamaillard^{1,2,3}, Claire Depardieu^{1,2,†}, Didier Le Thiec⁴, Hervé Cochard⁵, Têtè S. Barigah⁵ and Franck Brignolas^{1,2,‡}

¹ Université d'Orléans, UFR-Faculté des Sciences, UPRES EA 1207 Laboratoire de Biologie des Ligneux et des Grandes Cultures (LBLGC), BP 6759, F-45067, France

² INRA, USC1328 Arbres et Réponses aux Contraintes Hydriques et Environnementales (ARCHE), BP 6759, F-45067, France

³ INRA UR588 Amélioration, Génétique et Physiologie Forestières (AGPF), Centre de Recherche d'Orléans, CS 40001 Ardon, F-45075, Orléans Cedex 2, France

⁴ INRA, UMR1137 Ecologie et Ecophysiologie Forestières, Nancy Universités, IFR110 Génomique, Ecophysiologie, Ecologie Fonctionnelle, F-54280, Champenoux, France

⁵ UMR547 Physique et Physiologie Intégratives de l'Arbre Fruitier et Forestier (PIAF), INRA-Université Blaise Pascal, F-63100, Clermont-Ferrand, France

* Present address: University of Antwerp, Research Group of Plant and Vegetation Ecology, Department of Biology, Campus Drie Eiken, Universiteitsplein 1, B-2610, Wilrijk, Belgium

† Present address: Université de Franche-Comté, UMR UFC/CNRS 6249 USC INRA, Laboratoire Chrono-environnement, F-25030, Besançon, France

‡ To whom correspondence should be addressed. E-mail: franck.brignolas@univ-orleans.fr

Received 3 June 2010; Revised 15 November 2010; Accepted 17 November 2010

Abstract

Tests were carried out to determine whether variations in the hydraulic architecture of eight *Populus deltoides* × *Populus nigra* genotypes could be related to variations in leaf function and growth performance. Measurements were performed in a coppice plantation on 1-year-old shoots under optimal irrigation. Hydraulic architecture was characterized through estimates of hydraulic efficiency (the ratio of conducting sapwood area to leaf area, $A_X:A_L$); leaf- and xylem-specific hydraulic conductance of defoliated shoots, k_{SL} and k_{SS} , respectively; apparent whole-plant leaf-specific hydraulic conductance, k_{plant}) and xylem safety (water potential inducing 50% loss in hydraulic conductance). The eight genotypes spanned a significant range of k_{SL} from 2.63 kg s⁻¹ m⁻² MPa⁻¹ to 4.18 kg s⁻¹ m⁻² MPa⁻¹, variations being mostly driven by k_{SS} rather than $A_X:A_L$. There was a strong trade-off between hydraulic efficiency and xylem safety. Values of k_{SL} correlated positively with k_{plant} , indicating that high-pressure flowmeter (HPFM) measurements of stem hydraulic efficiency accurately reflected whole-plant water transport efficiency of field-grown plants at maximum transpiration rate. No clear relationship could be found between hydraulic efficiency and either net CO₂ assimilation rates, water-use efficiency estimates (intrinsic water-use efficiency and carbon isotope discrimination against ¹³C), or stomatal characteristics (stomatal density and stomatal pore area index). Estimates of hydraulic efficiency were negatively associated with relative growth rate. This unusual pattern, combined with the trade-off observed between hydraulic efficiency and xylem safety, provides the rationale for the positive link already reported between relative growth rate and xylem safety among the same eight *P. deltoides* × *P. nigra* genotypes.

Key words: high-pressure flowmeter (HPFM), hydraulic architecture, hydraulic conductance, relative growth rate, trade-offs, water relations, water-use efficiency, xylem vulnerability to cavitation.

Introduction

In higher plants, leaf water relations and ultimately growth are theoretically linked to plant hydraulic properties. This comes about because water flow through higher plants at steady state is generally well described by the Ohm's law analogue (Meinzer, 2002)

$$E = g_s \times \text{VPD} = k_{\text{plant}} \times (\psi_S - \psi_L) \quad (1)$$

where E is the leaf transpiration rate, g_s is the leaf stomatal conductance to water vapour, VPD is the leaf to air vapour pressure difference, k_{plant} is the leaf-specific hydraulic conductance of the whole plant, and ψ_S and ψ_L are the water potentials of the soil and the leaf, respectively. Experimental evidence suggests that the coordination between the liquid and vapour phase actually manifests at different scales. Within a given plant, numerous studies have demonstrated the active response of g_s to artificial modifications of k_{plant} (Meinzer and Grantz, 1991; Sperry *et al.*, 1993; Pataki *et al.*, 1998; Hubbard *et al.*, 2001; Cochard *et al.*, 2002). Across species, there is evidence that more efficient water transport at stem or leaf level allows both higher g_s and photosynthetic capacities as estimated from electron transport rates (Brodribb and Feild, 2000; Brodribb *et al.*, 2002, 2005) or net CO₂ assimilation rates (Santiago *et al.*, 2004; Brodribb *et al.*, 2007; Zhang and Cao, 2009). Further, maximum leaf hydraulic conductance has been found to be coordinated across species with leaf structure and stomatal pore area index (SPI = stomatal density \times guard cell length²) (Sack *et al.*, 2003, 2005), both of them influencing CO₂ diffusion within leaves and photosynthesis via mesophyll structure and stomata morphology. However, even if between-species comparisons indicate that high hydraulic efficiency is coordinated with a spectrum of leaf traits involved in carbon and water relations promoting faster growth, only a handful of studies have explicitly addressed the relationship between hydraulic efficiency, leaf traits, and growth performance at the intraspecific scale (Vander Willigen and Pammenter, 1998; Ducrey *et al.*, 2008).

Given the tight link between hydraulic efficiency and gas exchange rates, a relationship with water-use efficiency (WUE), a composite trait reflecting the balance between carbon gain and water loss, might also be expected. However, results gathered from between-species comparisons are conflicting. Recent comparisons of C₃ and C₄ species with consistently large differences in WUE have indicated that more water-use efficient C₄ species displayed lower leaf-specific hydraulic conductivity (Kocacinar and Sage, 2003, 2004; Kocacinar *et al.*, 2008). Other studies covering a broad range of species have reported similar trends between hydraulic efficiency and WUE (Sobrado, 2000; Drake and Franks, 2003; Sobrado, 2003; Santiago *et al.*, 2004), although such a relationship may be opposite (Campanello *et al.*, 2008) or absent (Preston and Ackerly, 2003; Edwards, 2006), possibly reflecting species-specific water-use strategies in different habitats. Actually, the link between WUE and hydraulic

efficiency remains poorly documented and unclear at the intraspecific scale (Panek, 1996; Ducrey *et al.*, 2008; Martínez-Vilalta *et al.*, 2009).

Beside hydraulic efficiency, xylem resistance to drought-induced cavitation is another key parameter for understanding the role of hydraulic architecture in leaf and whole-plant function (Sperry *et al.*, 2002). Functional coordination between xylem resistance to cavitation and leaf function may occur indirectly (Maherali *et al.*, 2006) through the combined effect of E and k_{plant} in determining the water potential drop from the soil to the leaves ($\Delta\Psi$) (see Equation 1). Indeed, large $\Delta\Psi$ generated by high E and/or low k_{plant} requires the construction of a safer xylem to prevent increased risks of embolism, and this generally translates into a trade-off between hydraulic efficiency and xylem resistance to cavitation. Therefore, the unique design of both k_{plant} and resistance to cavitation within a plant is supposed to be optimized so as to meet the conflicting balance between evaporative demand and safety from hydraulic failure (Tyree *et al.*, 1994).

Poplar species (*Populus* spp.) are widespread in the northern hemisphere and are known to be among the most superior angiosperm woody species in terms of growth rates under temperate latitudes (Heilman *et al.*, 1996). Because of large and positive heterosis effects for growth, poplar cultivation relies largely on the selection and the deployment of interspecific hybrids such as *Populus deltoides* Bartr. ex Marsh. \times *Populus nigra* L. Previous experiments undertaken on *P. deltoides* \times *P. nigra* genotypes have reported significant variation in juvenile growth potential and traits related to leaf water and carbon economy, including structural traits such as specific leaf area (SLA) or stomatal density, as well as functional traits such as leaf gas exchange rates and WUE (Marron *et al.*, 2005; Monclus *et al.*, 2005, 2006). More recent work has demonstrated that this suite of traits correlated with differences in xylem vessel anatomy (Fichot *et al.*, 2009), suggesting that one key to understanding the differences in growth behaviour and whole-plant water use may be vascular physiology.

The hypothesis that the hydraulic architecture is coordinated with leaf structural and functional traits as well as growth potential was tested in *P. deltoides* \times *P. nigra*. To answer this general objective, eight genotypes already known for differing widely in water use, growth behaviour, and xylem hydraulics (Monclus *et al.*, 2005, 2006; Fichot *et al.*, 2009, 2010) were selected. Measurements were performed on clonal copies of the eight genotypes grown in an open-field common garden under optimal irrigation, and included hydraulic traits (e.g. whole-stem and whole-plant hydraulic conductance, sapwood to leaf area ratio, and xylem resistance to cavitation), leaf structural and functional traits (e.g. gas exchange, WUE estimates, and SPI), and growth-related traits (relative growth rate). Specific objectives were to (i) examine the extent of genotypic variations in hydraulic efficiency; (ii) test the occurrence of a trade-off between hydraulic efficiency and

xylem resistance to cavitation; (iii) investigate the coordination of hydraulic efficiency with leaf gas exchange, WUE, and stomatal traits; and (iv) investigate the coordination between hydraulic efficiency and whole-plant growth performance.

Materials and methods

Plant material and experimental design

Experiments were performed in 2007 and 2008 on eight field-grown *P. deltoides* Bartr. ex Marsh × *P. nigra* L. genotypes already known for differing in water use, growth behaviour, and xylem hydraulics ('Agathe_F', 'Cima', 'Eco28', 'Flevo', 'I45-51', 'Luisa_Avanzo', 'Pannonia', and 'Robusta') (Monclus *et al.*, 2006; Fichot *et al.*, 2009, 2010). The plantation was located at Orléans (central France) within the INRA research station of Forest Genetics (47°46' N, 1°52' E, 110 m a.s.l.) and was set in June 2006 from 0.25 m long hardwood cuttings, on a loamy sand soil (pH 5.9) without addition of fertilizer. The experimental design consisted of a 250 m² coppice plantation split into two twin plots established 15 m apart from each other and separated by a no-man's land. Each plot was made up of eight north-south oriented rows and was divided into five complete randomized blocks with three individuals of each genotype per block. The initial spacing between individuals was 0.75 m within rows and 1.20 m between rows, accommodating an overall density of ~11 000 plants ha⁻¹. A border row of the cv. 'Mellone_Caro' was planted around each plot to minimize edge effects. All plants were cut back at the end of 2006 and 2007 to create a coppice system.

All experiments were carried out in 2007 and 2008; each year, bud-flush occurred synchronously within the first 2 weeks of April. Environmental conditions (cumulative precipitations, temperature, and potential evapotranspiration) were recorded on an hourly basis during the two years using a meteorological station (Xaria, Degreane Horizon, Cuers, France) located in the field site. The mean annual temperature was 11.2 °C and 10.5 °C in 2007 and 2008, respectively, the coldest month being December (3.8 °C and 2.1 °C, respectively) and the warmest, July (17.7 °C and 18.5 °C, respectively). The cumulative annual precipitation was 796 mm in 2007 and 532 mm in 2008, with ~50% occurring during the growing period (April–September). For both years, irrigation was performed using overhead sprinklers and was designed to meet the evaporative demand (i.e. 4.5 mm were sprinkled every time cumulative evapotranspiration reached 4 mm). However, in 2008, one of the two plots served as a water deficit experiment by withholding irrigation from 18 June to the end of the growing season, as described in detail in Fichot *et al.* (2010). Therefore, all measurements performed in 2008 after 18 June were conducted on the irrigated plot only.

High-pressure flowmeter (HPFM) measurements

Measurements of shoot hydraulic conductance were performed in the first 2 weeks of June in 2007 and 2008 to minimize genotypic differences in overall shoot size. Dominant shoots were selected over the two plots and at least one shoot of each genotype per block was sampled. Shoots were collected in batches of 4–6 so that subsequent hydraulic measurements were completed within a maximum of 2.5 h after sampling. In the field, individual leafy shoots were cut at their base with pruning shears. To minimize xylem tension at the time of sampling, tap water was sprayed on transpiring leaves. The cut ends of the shoots were immediately immersed in water and shoots were transported to a nearby glasshouse. The cut ends of the shoots were refreshed under water with a fresh razor blade and connected to the hydraulic apparatus for measurement via a compression fitting.

Measurements of hydraulic conductance were performed using a home-made HPFM (see Tyree *et al.*, 1995) under glasshouse irradiance conditions between 07:00 h and 17:00 h solar time. Since the hydraulic conductance of leaves is prone to rapid irradiance-induced variations (Tyree *et al.*, 2005; Cochard *et al.*, 2007a), only values of stem hydraulic conductance are reported in this study. Measurements were performed in the quasi-steady-state mode (i.e. maintaining the pressure applied approximately constant). Shoots were first perfused with degassed and filtered (0.1 µm) ultra-pure water at a pressure of 0.3 MPa (*P*) until water dripped from the stomata, which typically took 20–30 min. This was assumed to be sufficient to ensure zero water potential in the whole shoot and to dissolve air bubbles from potentially embolized xylem vessels. The hydraulic resistance of the stem (*r_s*) was then recorded after severing all leaves following the procedure described by Yang and Tyree (1994). Water flow rate (*F*, kg s⁻¹) was recorded every 4 s until values stabilized (i.e. coefficient of variation <5% within a few minutes) and *r_s* was computed from quasi steady-state parameters as the ratio between *P* and *F*. The stem hydraulic conductance (*k_s*, kg s⁻¹ MPa⁻¹) was then computed as the inverse of the stem hydraulic resistance and standardized to 20 °C as $k_{s=20} = v/v_0 \times (1/r_s)$ where *v* and *v₀* are the kinematic viscosities of water at the measured temperature and 20 °C, respectively.

Shoot total leaf area (*A_L*, m²) and xylem cross-sectional area of the stem (*A_X*, m²) were determined for each sampled shoot. *A_L* was determined using a Li-Cor 3000-A area meter (equipped with a Li-Cor Belt Conveyor 3050-A; Li-Cor Instruments, Lincoln, NE, USA) immediately after determination of hydraulic conductance. *A_X* was determined by analysing digital images of 30 µm thick basal cross-sections and subtracting the pith area (VISILOG 6.3 software, Noesis, St Aubain, France). The leaf-specific hydraulic conductance of the stem (*k_{SL}*, kg s⁻¹ m⁻² MPa⁻¹) was calculated as *k_s* divided by *A_L*. The xylem-specific hydraulic conductance (*k_{SS}*, kg s⁻¹ m⁻² MPa⁻¹) was calculated by dividing *k_s* by *A_X*. The ratio *A_X:A_L* was used as a morphological index of potential water transport capacity to transpirational demand; this ratio is the relational product linking *k_{SS}* to *k_{SL}* (Tyree and Ewers, 1991).

Xylem resistance to cavitation

Data for xylem resistance to cavitation were obtained from a previous study performed on the same field trial (Fichot *et al.*, 2010). Briefly, five dominant shoots per genotype (one per block) were sampled on the well-watered plot at the end of the 2008 growing season and were processed as described in Fichot *et al.* (2010). The recently developed Cavitrone technique (Cochard *et al.*, 2005), an method adapted from the centrifuge technique (Alder *et al.*, 1997), was used to generate vulnerability curves. The xylem tension causing 50% loss in hydraulic conductance (*Ψ₅₀*) was derived from these curves and used as an index of the resistance to xylem cavitation (Fichot *et al.*, 2010).

Leaf gas exchange, water potentials, and whole-plant hydraulic conductance

Net CO₂ assimilation rate (*A*, µmol m⁻² s⁻¹), stomatal conductance to water vapour (*g_s*, mmol m⁻² s⁻¹), and transpiration rate (*E*, mmol m⁻² s⁻¹) were assessed the same day for all genotypes using a portable gas exchange system (LI-6200; Li-Cor) between 11:00 h and 13:00 h local time in July 2008, as described in Fichot *et al.* (2010). Measurements were made on one fully illuminated mature leaf (foliar rank of 15 or 16 counting from the first top leaf exceeding 20 mm in length) on the main shoot of one individual per genotype per block (*n*=5 per genotype). Leaf temperature (mean 27.6±0.2 °C), VPD (mean 1.7±0.1 kPa), and photosynthetic photon flux density (1378±55 µmol s⁻¹ m⁻²) matched ambient conditions. The leaves were allowed to equilibrate inside the chamber for 20 s before measurements were taken. Intrinsic

WUE (WUE_i, mmol mol⁻¹) was then calculated as the ratio between A and g_s .

Midday leaf water potential (Ψ_L , MPa) and pre-dawn leaf water potential (Ψ_{pd} , MPa) were measured with a pressure chamber (PMS Instruments, Albany, OR, USA) and used to estimate the apparent leaf area-specific whole-plant hydraulic conductance (k_{plant} , kg s⁻¹ m⁻² MPa⁻¹). Ψ_L was measured on the same leaves used for leaf gas exchange and was assumed to equate to the minimum Ψ_L diurnal values. To prevent errors due to rapid water loss once leaves were removed, leaves were placed in small plastic bags with a moist towel, placed on ice, and transported to a nearby laboratory installed on the field plot where they were rapidly processed for Ψ_L . Ψ_{pd} was assessed over each block on a subset of three genotypes the day preceding and the day after gas exchange measurements. Values of k_{plant} ($n=5$, one per plot) were calculated on the basis of the Ohm's law analogy as $k_{plant}=E/(\Psi_{pd}-\Psi_L)$ using individual Ψ_L values and mean block Ψ_{pd} values over the two days of measurements.

Stomatal density, guard cell length, and stomatal pore area index

Three discs of leaf lamina (1 cm² each) from the leaves used for gas exchange and Ψ_L were punched centrally, midway between the midrib and margin, and stored at -20 °C until they were processed. Samples were then stuck to aluminium stubs on a Peltier stage (-50 °C) before being examined under a controlled-pressure scanning electron microscope (model 1450VP, Leo, Cambridge, UK; 20–30 Pa inside the chamber, accelerating voltage 15 kV, working distance 12 mm). Microphotographs were then taken and processed using image analysis software (VISILOG). Because poplar leaves are amphistomatous, each disc was split in half for the separate analysis of leaf adaxial and abaxial sides, respectively. Stomatal density and stomatal pore length were measured on each half disc from one digital image taken at $\times 400$ and $\times 1200$ magnifications, respectively. Counts and measurements were then averaged for the three discs so that 18 stomata per leaf were used for estimating stomatal pore length. The total stomatal density was calculated as the sum of the adaxial and abaxial stomatal densities. The total SPI (a theoretical index of maximum stomatal conductance) was calculated as the mean total stomatal density \times mean stomatal pore length² (Sack *et al.*, 2003).

Specific leaf area, nitrogen content, and carbon isotope discrimination against ¹³C

SLA (cm² g⁻¹), nitrogen content (N_M , g g⁻¹), and carbon isotope discrimination against ¹³C (Δ , ‰) were assessed in July 2008 from the same leaves used to measure gas exchange parameters in order to validate the functional relationship between Δ and WUE_i. Six discs of leaf lamina (2 cm² each) were punched from each leaf and oven-dried at 60 °C until constant mass (24 h), allowing the calculation of SLA. The six discs of leaf lamina were then ground to a fine powder and used for the determination of bulk leaf ¹³C isotope composition ($\delta^{13}C$) and nitrogen content. Analyses were performed at the technical platform of functional ecology at the INRA research station of Nancy (France). Each 1 mg subsample of ground material was enclosed in a tin capsule and combusted. The CO₂ produced by combustion was purified and its ¹³CO₂/¹²CO₂ ratio was analysed with a Finnigan MAT Delta S isotope ratio mass spectrometer (IRMS) (Bremen, Germany). Carbon isotope composition was expressed relative to the Pee Dee Belemnite (PDB) standard and was calculated as:

$$\delta^{13}C = [(R_{sa} - R_{sd})/R_{sd}] \times 1000 \text{ (‰)} \quad (2)$$

where R_{sa} and R_{sd} are the ¹³CO₂/¹²CO₂ ratios of the sample and the standard, respectively (Farquhar *et al.*, 1989). The accuracy of $\delta^{13}C$ measurements during the time samples were passed on the IRMS was $\pm 0.15\%$ (SD). The carbon isotope discrimination (Δ)

between atmospheric CO₂ (δ_{air}) and plant material (δ_{plant}) was then calculated as:

$$A = (\delta_{air} - \delta_{plant}) / [1 + (\delta_{plant}/1000)] \quad (3)$$

assuming δ_{air} equals -8‰ (Farquhar *et al.*, 1989). The time-integrated intercellular CO₂ concentration (C_i) was obtained by rearranging the equation for carbon isotope ratio from Farquhar *et al.* (1982) to give:

$$C_i = c_a(\delta_{air} - \delta_{plant} - a) / (b - a) \quad (4)$$

where c_a is the atmospheric CO₂ concentration (380 ppm), a is the fractionation caused by diffusion (4.4‰), and b is the net fractionation caused by Rubisco carboxylation (27‰). The nitrogen concentration of the same samples used for $\delta^{13}C$ analyses was obtained with a Carlo Erba NAI500 elemental analyser (Carlo Erba Instruments, Milan, Italy) coupled to the IRMS and was expressed on a dry mass basis (N_M , g g⁻¹).

Whole-plant growth performances

Whole-plant growth performance was characterized for each genotype by computing the relative growth rate (RGR, g g⁻¹ day⁻¹) of the main shoot of each stool during the 2008 growing season ($n=15$ per genotype). This was realized by combining seasonal growth kinetics in terms of shoot height increment and allometric relationships established between shoot height and shoot dry mass for each genotype, as described in detail in Fichot *et al.* (2010). The RGR was calculated for a time period of linear growth common to the eight genotypes as $RGR = [\ln(m_2) - \ln(m_1)] / (t_2 - t_1)$, where m_1 and m_2 are the estimated shoot dry mass at t_1 (4 July) and t_2 (14 August), respectively (Fichot *et al.*, 2010).

Statistical analyses

All analyses were performed using analysis of variance (ANOVA) with individual block values used as replicates. For HPFM data, when data were available for more than one individual per block and per genotype, values were averaged to give a single genotypic block value. In preliminary analyses, the block effect was included as a fixed effect in each model. When no significant block effect was found, the factor block was then removed from the model. In cases where the factor block was significant (i.e. for g_s , WUE_i, and c_i ; $P < 0.05$), individual values were adjusted to block effects by calculating the difference between the mean of each block and the general mean over the eight genotypes (e.g. Dillen *et al.*, 2008, 2009). To account for a possible year effect for HPFM measurements, the model used for HPFM data was

$$var = \text{Geno} + \text{Year} + (\text{Geno} \times \text{Year})$$

where 'var' refers to the tested variable (A_X : A_L , k_{SL} , or k_{SS}), 'Geno' refers to the genotype effect considered as random, 'Year' refers to the year effect (2007 or 2008) considered as fixed, and '(Geno \times Year)' refers to the genotype by year interaction. To test genotype and year effects on k_{SL} and k_{SS} independently of plant size, either A_X or A_L was added as covariate to the model. As foliar and growth data were only available for 2008, a simplified one-way ANOVA model was run to account only for genotype effect. Relationships between pairs of continuous variables were analysed by linear regression analysis [Pearson's correlation coefficients (r)] using genotypic means. Data management and statistical analyses were carried out using the SPSS 11.0 statistical software (SPSS, Chicago, IL, USA). Curve fitting and graph handling were performed using Sigmaplot (version 8.0, SPSS Inc., San Rafael, CA, USA). All tests were considered significant at $P < 0.05$. Genotypic means are expressed with their standard errors. Standard errors for genotypic means based on 2007+2008 data (HPFM data) were derived from standard rules of error propagation.

Results

Hydraulic variables

For all genotypes there was a highly significant ($Geno \times Year$) interaction for k_{SL} and k_{SS} values (Table 1). Further analysis indicated that interactions were mainly driven by ‘Luisa_Avanzo’ for which 2007 and 2008 values were strikingly different (Table 1, Fig. 1). When this genotype was discarded from the analysis, there was a significant $Geno$ effect for $A_X:A_L$, k_{SL} , and k_{SS} , a significant $Year$ effect for $A_X:A_L$ and k_{SL} , but no significant ($Geno \times Year$) interactions (Table 1). HPFM data for ‘Luisa_Avanzo’ were therefore discarded from all subsequent analyses and data for $A_X:A_L$, k_{SL} , and k_{SS} were averaged over 2007 and 2008 for each of the remaining seven genotypes.

A_X and A_L , expressed in m^2 , scaled positively at the genotype level [$A_X = 2.10^{-4} \times A_L = 4.10^{-6}$; $r=0.83$, $P=0.021$; ($n=7$)]. k_{SL} and k_{SS} were highly correlated, while no significant correlation could be found between k_{SL} and $A_X:A_L$ (Fig. 2A,B). The calculated k_{plant} varied significantly among genotypes ($P < 0.001$) and scaled positively with k_{SL} (Fig. 2C). As expected, k_{plant} was about two orders of magnitude lower than k_{SL} since k_{plant} integrates the hydraulic resistance of both roots and leaves.

Vulnerability curves for the eight genotypes grown under non-limiting conditions were already available from a previous experiment (Fichot *et al.*, 2010); the analysis revealed that values of Ψ_{50} varied significantly ($P < 0.001$) among genotypes from -1.60 MPa for ‘Robusta’ to -2.41 MPa for ‘Eco28’. $|\Psi_{50}|$ scaled negatively with k_{SL} , k_{SS} , and k_{plant} ; that is, the greater the resistance to cavitation, the lower the efficiency of water transport (Fig. 3).

Leaf characteristics and relationships with hydraulic architecture

Significant variations ($P < 0.05$) were found among genotypes for all leaf structural and functional traits (Table 2). Values of Ψ_L were constrained in a narrow range (-1.48 MPa to -1.92 MPa; Table 2) and did not correlate

Table 1. Analysis of variance (ANOVA) probability values for genotype (Geno), year (Year) and genotype by year ($Geno \times Year$) effects on xylem area to leaf area ratio ($A_X:A_L$), leaf-specific hydraulic conductance (k_{SL}), and xylem-specific hydraulic conductance (k_{SS})

ANOVA results are presented for all genotypes gathered ($n=8$) and after excluding ‘Luisa_Avanzo’ from the analysis ($n=7$).

	ANOVA all genotypes			ANOVA excluding ‘Luisa_A’		
	Geno	Year	Geno×Year	Geno	Year	Geno×Year
$A_X:A_L$	0.076	0.006	0.061	0.010	<0.001	NS
k_{SL}	NS	0.071	<0.001	0.007	0.021	NS
k_{SS}	NS	NS	<0.001	0.002	0.097	NS

The probability level $P < 0.10$ was considered to indicate a trend.

significantly with either A or g_s ($P > 0.927$). A did not correlate significantly with either g_s ($r=0.45$, $P=0.259$), SLA ($r=0.22$, $P=0.605$), or N_M ($r=0.43$, $P=0.282$). Variations in WUE_i were mostly driven by g_s ($r = -0.94$, $P < 0.001$) rather

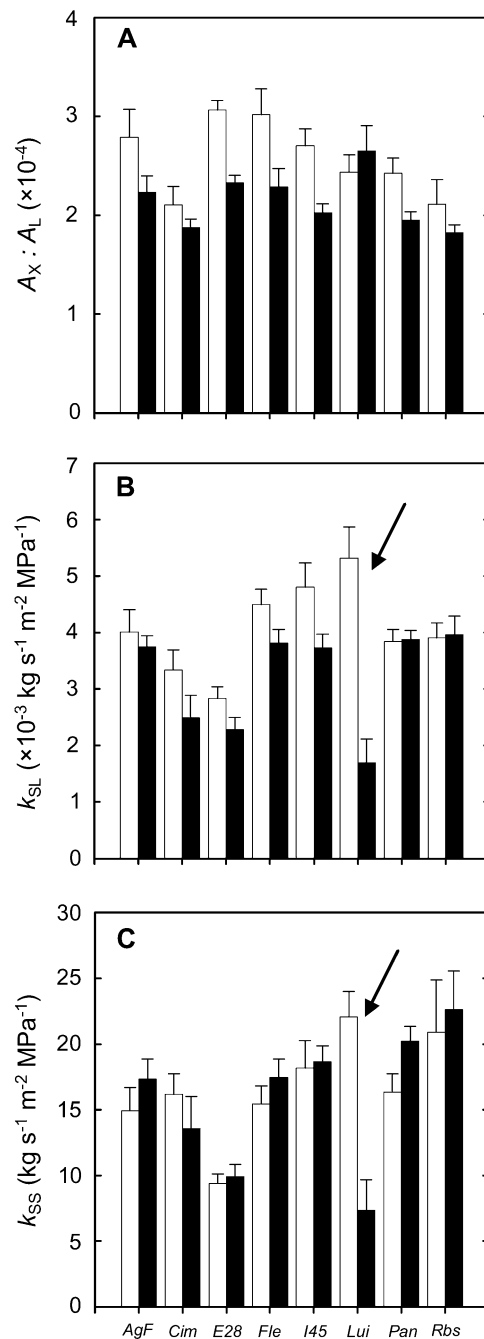


Fig. 1. Mean genotypic values for sapwood area to leaf area ratio ($A_X:A_L$), leaf-specific hydraulic conductance (k_{SL}), and xylem-specific hydraulic conductance (k_{SS}) assessed in 2007 (open bars) and 2008 (filled bars) for the eight *Populus deltoides* × *P. nigra* genotypes. Values are means \pm SE. Please note the important differences between years for k_{SL} and k_{SS} in the genotype ‘Luisa_Avanzo’ (*Lui*). Genotype abbreviations: *Ag_F*, ‘Agathe_F’; *Cim*, ‘Cima’; *E28*, ‘Eco28’; *Fle*, ‘Flevo’; *I45*, ‘I45-51’; *Lui*, ‘Luisa_Avanzo’; *Pan*, ‘Pannonia’; *Rbs*, ‘Robusta’.

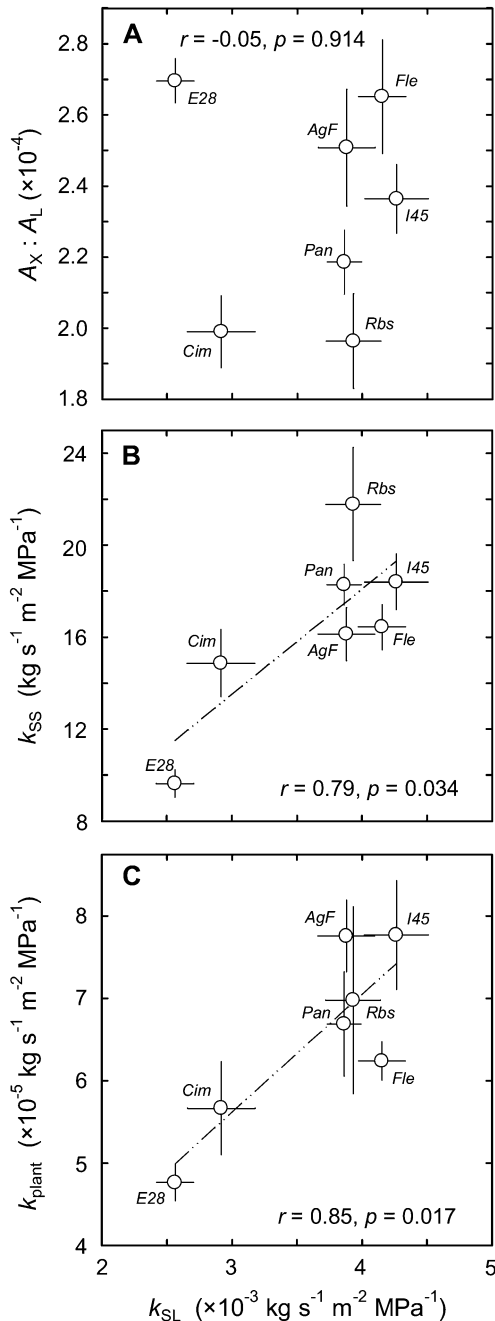


Fig. 2. The relationship between leaf-specific hydraulic conductance of the stem as measured with the HPMF (k_{SL}) and (A) sapwood to leaf area ratio ($A_x:A_L$), (B) xylem-specific hydraulic conductance (k_{SS}), and (C) apparent whole-plant leaf-specific hydraulic conductance as calculated from the Ohm's law analogy (k_{plant}). Values are genotypic means \pm SE (values for k_{SL} and k_{SS} represent genotypic means over 2007 and 2008). The dash-dotted lines are significant linear regressions fitted to the data (Pearson's correlation coefficients, r). Genotype abbreviations are as in Fig. 1.

than by A ($r = -0.15$, $P = 0.723$). Similarly, variations in Δ were mostly driven by g_s ($r = 0.62$, $P = 0.103$) rather than by A ($r = -0.08$, $P = 0.860$). A significant linear and negative relationship was found between Δ and WUE_i , as expected from theory (Fig. 4A). Additionally, there was a significant and positive relationship between c_i derived

from instantaneous leaf gas exchange measurements and C_i derived from time-integrated Δ analyses, although c_i was 11–24% higher than C_i (Fig. 4B). No significant relationship could be found between Δ and SLA ($r = 0.61$, $P = 0.111$).

Stomatal density varied ~ 2 -fold, from 151 mm^{-2} in 'I45-51' to 333 mm^{-2} in 'Eco28' ($P < 0.001$), and stomatal pore length varied from $18.5 \mu\text{m}$ in 'Cima' to $24.9 \mu\text{m}$ in 'I45-51' ($P < 0.001$) (Table 2). Stomatal density decreased with increasing stomatal pore length ($r = -0.76$, $P = 0.027$) but no longer when 'I45-51' was discarded from the analysis ($r = 0.035$, $P = 0.941$), suggesting that this genotype was mainly responsible for the relationship. Additionally, the relationship between stomatal density and stomatal pore length was not sufficiently compensatory to equalize SPI (the product of stomatal density and stomatal pore length²) so that SPI varied significantly among the eight genotypes ($P < 0.001$) from 8.9×10^{-2} in 'Cima' to 13.2×10^{-2} in 'Eco28' (Table 2). Variations in stomatal density were mostly responsible for the variations observed in SPI ($r = 0.73$, $P = 0.039$), while variations in stomatal pore length contributed poorly ($r = -0.13$, $P = 0.757$). Stomatal density correlated significantly and negatively with g_s and Δ , and positively with WUE_i (Fig. 5A–C); the same trends were observed with SPI though the relationships were stronger (Fig. 5D,–F). There were no significant correlations between stomatal pore length and either g_s , Δ , or WUE_i ($P > 0.410$).

There was no significant relationship between Ψ_L and either k_{SL} or $|\Psi_{50}|$ ($P > 0.270$). Neither g_s nor A was significantly related to k_{SL} (Fig. 6), although g_s and $|\Psi_{50}|$ were significantly and negatively related to each other ($r = 0.78$, $P = 0.021$; Fichot *et al.*, 2010). WUE estimates were not significantly related to k_{SL} (Fig. 6). Similarly, stomatal characteristics (stomatal density, stomatal pore length, and SPI) did not scale significantly with estimates of hydraulic efficiency ($P > 0.150$).

Relative growth rate and relationships with hydraulic architecture

Growth potential as inferred from the RGR varied markedly among the eight genotypes, from $0.013 \text{ g g}^{-1} \text{ d}^{-1}$ for 'Robusta' to $0.035 \text{ g g}^{-1} \text{ d}^{-1}$ for 'Eco28' ($P < 0.001$; Fig. 7). There were no significant relationships between the RGR and gas exchange parameters such as g_s ($r = -0.41$, $P = 0.312$), A ($r = -0.45$, $P = 0.263$), and WUE as inferred from WUE_i ($r = 0.37$, $P = 0.365$) or Δ ($r = -0.19$, $P = 0.653$), as already reported by Monclus *et al.* (2006) on the same set of genotypes under a comparable environment. The RGR scaled negatively with k_{SL} , k_{SS} , and k_{plant} ; that is, the more the relative growth performed well, the less efficient was water transport (Fig. 7). As k_{SL} , k_{SS} , and k_{plant} varied negatively with $|\Psi_{50}|$, the RGR scaled significantly and positively with $|\Psi_{50}|$; that is, the more the relative growth performed well, the greater was the resistance to cavitation ($r = 0.82$, $P = 0.009$; Fichot *et al.*, 2010).

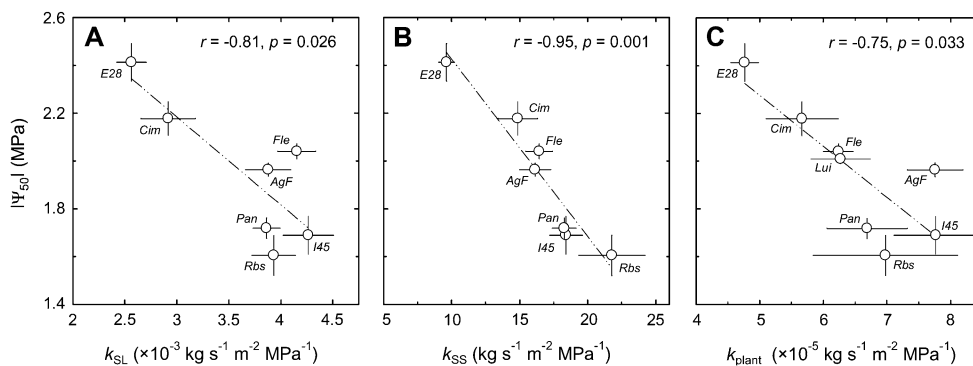


Fig. 3. The xylem tension causing 50% loss in stem hydraulic conductance (Ψ_{50}) as a function of (A) leaf-specific hydraulic conductance (k_{SL}), (B) xylem-specific hydraulic conductance (k_{SS}), and (C) apparent whole-plant leaf-specific hydraulic conductance (k_{plant}). Note that negative Ψ_{50} data were converted to absolute values. Values are genotypic means \pm SE (values for k_{SL} and k_{SS} represent genotypic means over 2007 and 2008). The dash-dotted lines are linear regressions fitted to the data (Pearson's correlation coefficients, r). Genotype abbreviations are as in Fig. 1.

Table 2. Summary of leaf structural, morphological, and functional characteristics for the eight genotypes

	Genotypes							
	AgF	Cim	E28	Fle	I45	Lui	Pan	Rbs
SLA ($\text{cm}^2 \text{g}^{-1}$)	116.9 (2.4)	119.2 (4.0)	97.4 (2.5)	112.2 (6.4)	106.3 (2.6)	120.4 (2.7)	111.8 (2.0)	114.7 (2.9)
N_{mass} (g g^{-1})	0.020 (0.000)	0.017 (0.001)	0.017 (0.001)	0.021 (0.001)	0.017 (0.001)	0.019 (0.001)	0.023 (0.002)	0.019 (0.002)
Ψ_L (MPa)	-1.57 (0.05)	-1.92 (0.13)	-1.69 (0.07)	-1.51 (0.08)	-1.48 (0.06)	-1.51 (0.06)	-1.72 (0.06)	-1.84 (0.11)
A_{area} ($\mu\text{mol s}^{-1} \text{m}^{-2}$)	18.1 (1.3)	15.0 (0.8)	13.8 (1.0)	13.5 (0.9)	15.9 (0.5)	14.4 (1.1)	17.9 (0.7)	14.9 (0.9)
g_s ($\text{mmol s}^{-1} \text{m}^{-2}$)	502 (54)	582 (52)	365 (77)	441 (33)	708 (52)	609 (92)	674 (25)	605 (45)
E ($\text{mmol s}^{-1} \text{m}^{-2}$)	6.5 (0.2)	5.4 (0.6)	4.0 (0.3)	4.9 (0.4)	5.8 (0.4)	4.6 (0.3)	5.7 (0.4)	6.3 (0.9)
c_i (ppm)	308.7 (4.9)	323.8 (13.0)	280.7 (12.4)	284.6 (6.8)	316.4 (2.4)	310.5 (1.9)	314.9 (9.9)	310.7 (9.7)
WUE_i (mmol mol^{-1})	0.037 (0.002)	0.027 (0.001)	0.043 (0.006)	0.034 (0.001)	0.021 (0.003)	0.025 (0.004)	0.026 (0.002)	0.025 (0.003)
Δ (‰)	19.94 (0.22)	21.26 (0.16)	19.88 (0.27)	19.77 (0.13)	20.90 (0.16)	20.49 (0.08)	20.09 (0.20)	21.07 (0.24)
Total stomatal density (mm^{-2})	310 (10)	260 (13)	333 (7)	270 (17)	151 (6)	276 (14)	279 (10)	230 (8)
Stomatal pore length (μm)	19.3 (0.2)	18.5 (0.7)	19.9 (0.6)	21.0 (0.4)	24.9 (0.7)	19.4 (0.8)	19.6 (0.3)	19.8 (0.7)
Total SPI	0.116 (0.006)	0.089 (0.007)	0.132 (0.007)	0.119 (0.010)	0.094 (0.002)	0.104 (0.008)	0.107 (0.006)	0.090 (0.005)

Values are means (\pm SE) ($n=5$).

A_{area} , area-based net CO_2 assimilation rate; c_i , instantaneous intercellular CO_2 concentration; E , leaf transpiration rate; g_s , stomatal conductance to water vapour; N_{mass} , mass-based nitrogen content; SLA, specific leaf area; SPI, stomatal pore area index; WUE_i , intrinsic water-use efficiency; Δ , bulk leaf carbon isotope discrimination; Ψ_L , midday leaf water potential. See Fig. 1 for genotype abbreviations.

Discussion

Hydraulic architecture

Significant variations in hydraulic efficiency were found among the studied *P. deltoides* × *P. nigra* genotypes. Values recorded for k_{SL} and k_{SS} were generally at least one order of magnitude higher than those reported in other deciduous and evergreen forest tree species (Nardini and Tyree, 1999; Nardini and Salleo, 2000; Nardini, 2001; Caquet *et al.*, 2009), but they were quite comparable with those found among four closely related willow clones (Wikberg and Ögren, 2004). High hydraulic efficiency combined with high rates of water loss and net carbon fixation are characteristic of pioneer tree species (Tyree *et al.*, 1998; Becker *et al.*, 1999; Sobrado, 2003). Thus, the high values of k_{SL} and k_{SS} recorded in the present study, combined with an overall high vulnerability to drought-induced embolism, are related to the pioneering and opportunistic behaviour of poplar.

Measurements of k_{SL} reported herein only account for the stem hydraulic resistance, and are actually maximal values since the positive pressures used by the HPFM are likely to refill embolized vessels and to eliminate effects of water capacitance (Tyree *et al.*, 1995). In contrast, field measurements of k_{plant} integrate by definition all soil-to-leaf hydraulic resistances, potential emboli, as well as possible non-steady-state water flow. In spite of inherent differences between the two types of measurements, the tight relationship between k_{SL} and k_{plant} indicated that HPFM measurements of stem hydraulic efficiency accurately reflected whole-plant water transport efficiency of field-grown plants at maximum transpiration rate. This pattern is, however, to be expected only if the water transport pathway is coordinated at different points in the entire transport pathway from roots to leaves; that is, only if higher stem hydraulic efficiency scales to some extent to higher root and leaf hydraulic efficiency (see discussion in Sack *et al.*, 2005; Pratt *et al.*, 2010).

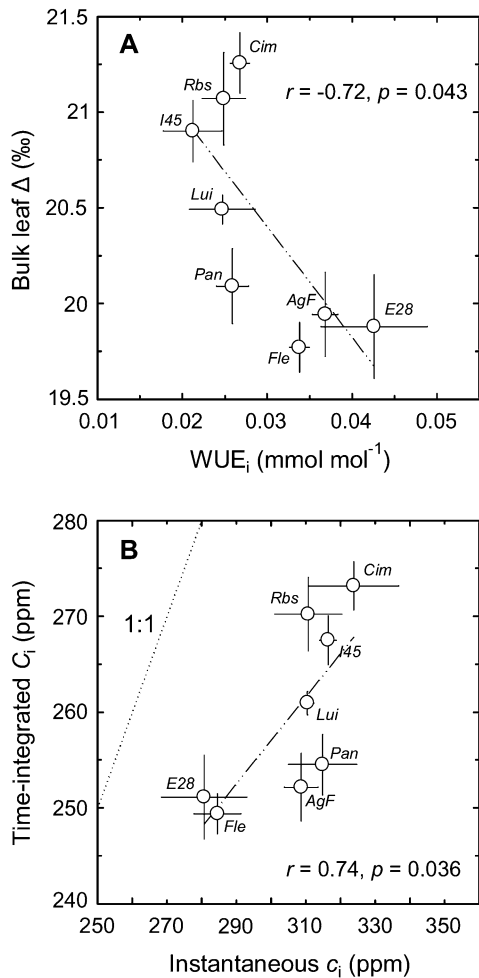


Fig. 4. Relationships between time-integrated and instantaneous characteristics of water-use efficiency (WUE). (A) Bulk leaf carbon isotope discrimination (Δ) as a function of intrinsic water-use efficiency (WUE_i). (B) Time-integrated intercellular CO_2 concentration calculated from Δ data (C_i) as a function of instantaneous intercellular CO_2 concentration obtained from gas exchange measurements (c_i). Values are genotypic means \pm SE ($n=5$). The dash-dotted lines are linear regressions fitted to the data (Pearson's correlation coefficients, r). The dotted line in (B) indicates the 1:1 relationship. Genotype abbreviations are as in Fig. 1.

By definition, k_{SL} is the product of k_{SS} and $A_X:A_L$ (Tyree and Ewers, 1991). In this study, k_{SL} was strongly and linearly related to k_{SS} but not to $A_X:A_L$, indicating that differences in stem xylem anatomy were mainly responsible for the variability observed in leaf-specific hydraulic efficiency rather than differences in patterns of carbon partitioning between xylem tissue and canopy area. However, the exact structural basis for increased k_{SS} in genotypes with higher k_{SL} was not directly addressed in this study. The axial xylem hydraulic conductance is intrinsically dependent on the number of conduits in parallel, their diameter, and their length (Tyree and Zimmermann, 2002). A previous study demonstrated significant variations in stem vessel diameter and vessel frequency among six out of

the eight study genotypes (Fichot *et al.*, 2009), but vessel attributes from this study did not correlate significantly with HPFM estimates of hydraulic efficiency (data not shown). A probable explanation may relate to the fact that estimating xylem hydraulic efficiency using cross-sectional vessel characteristics ignores some key aspects of water flow efficiency in contrast to HPFM measurements, such as (i) vessel lengths and contribution of end walls to hydraulic resistance (Sperry *et al.*, 2005; Wheeler *et al.*, 2005); and (ii) spatial patterns of conduit ramification and tapering from the base to the top of the stem (McCulloh *et al.*, 2010).

There was evidence for a trade-off between water transport efficiency and xylem safety, consistently with other studies reporting such trade-off at the organ or at the whole-plant level (e.g. Hacke *et al.*, 2000; Martínez-Vilalta *et al.*, 2002; Bucci *et al.*, 2006; Maherali *et al.*, 2006; Pratt *et al.*, 2007). At the whole-plant level, a common explanation for this trade-off relates to the fact that a lower k_{SL} or k_{plant} at any given transpiration rate is expected to result in a larger potential drop ($\Delta\Psi$) along the soil-to-leaf hydraulic continuum and thus requires the construction of a safer xylem to circumvent the greater risks of embolism. However, ideal optimization of the conflicting balance between water transport efficiency and safety from hydraulic failure would translate into rather low and conserved safety margins across genotypes. Instead, the difference between stem water potential at maximal transpiration and the water potential inducing significant embolism (the so-called safety margin) varied significantly among the eight genotypes (from 0.98 MPa to -0.02 MPa; see Fichot *et al.*, 2010) which contrasts with the common observation that similar and low safety margins tend to be conserved across a broad range of species and habitats (Hacke *et al.*, 2000; Jacobsen *et al.*, 2007; Pratt *et al.*, 2007). The functional significance of such variable safety margins within *P. deltoides* \times *P. nigra* remains therefore unclear under non-limiting conditions, but this trend is likely to translate into different growth and water-use strategies during short water shortages.

Coordination between hydraulic architecture and leaf function

One corollary objective of this study was to test whether the coordination between the liquid and vapour phase predicted from the Ohm's law analogue for fluid flow (Equation 1) and supported by a large body of interspecific studies (Brodribb and Feild, 2000; Brodribb *et al.*, 2002, 2005; Santiago *et al.*, 2004; Zhang and Cao, 2009) held across the *P. deltoides* \times *P. nigra* genotypes. The loose relationship observed between k_{SL} and g_s when considering all genotypes suggested at first that the coordination may not be inherent in all cases, with genotypes not necessarily falling on a single relationship. Excluding 'Flevo' from the analysis resulted, however, in a more or less straightforward relationship between k_{SL} and g_s across the remaining genotypes. It is unlikely that uncertainties in gas exchange measurements were responsible for the deviation in the k_{SL}/g_s coordination as (i) WUE_i data correlated negatively

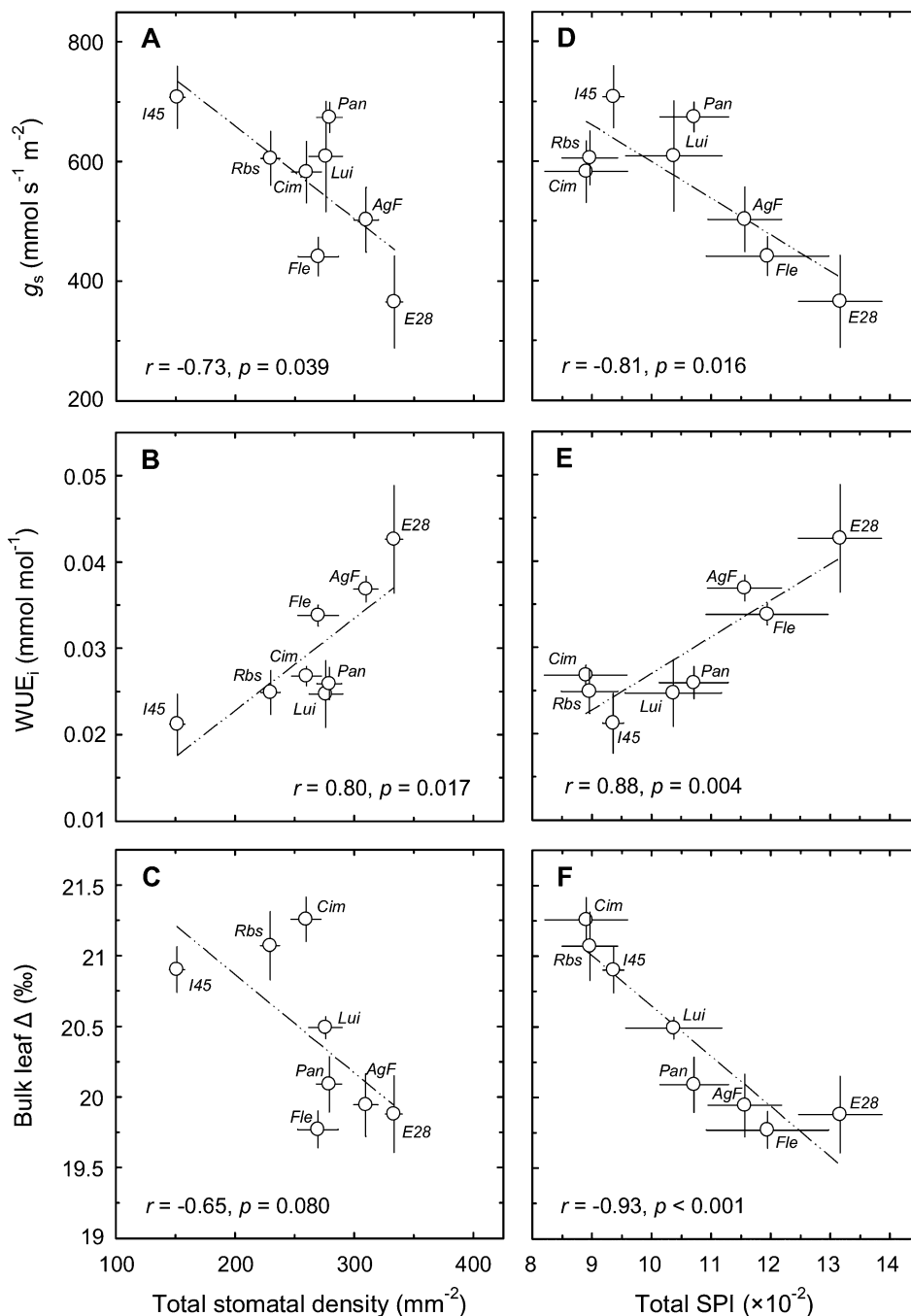


Fig. 5. Stomatal conductance (g_s), intrinsic water-use efficiency (WUE_i), and bulk leaf carbon isotope discrimination (Δ) as a function of total stomatal density (A–C) or total stomatal pore area index (SPI) (D–F). Values are genotypic means \pm SE ($n=5$). The dash-dotted lines are linear regressions fitted to the data (Pearson's correlation coefficients, r). Genotype abbreviations are as in Fig. 1.

with time-integrated Δ data as expected from theory; and (ii) g_s and $|\Psi_{50}|$ were negatively and tightly related ($r=0.78^*$; see Fichot *et al.*, 2010) as already reported across a wide range of Angiosperm species (Maherali *et al.*, 2006). Rather, it is noteworthy that 'Flevo' shoots tended to exhibit more sylleptic branchiness with small-sized leaves as compared with other genotypes (RF, unpublished observations) which may have contributed to overestimating k_{SL} for this particular genotype and to bring some scatter in the k_{SL}/g_s relationship. This line of reasoning is supported by the fact that 'Flevo' was frequently out of range as compared with the other

genotypes when examining the relationships between k_{SL} and other variables (see for instance Figs 2 and 3).

No evidence was found for a relationship between hydraulic efficiency and WUE_i , as inferred from WUE_i and Δ . It should be stressed that, although not significant, the relationships between estimates of hydraulic efficiency and WUE_i tended to be stronger than with Δ . This trend may be easily explained considering that HPFM and WUE_i estimates are based on steady-state measurements ignoring the dynamic responses of liquid and vapour phase conductance (Tsuda and Tyree, 2000; Meinzer, 2002), in contrast to Δ

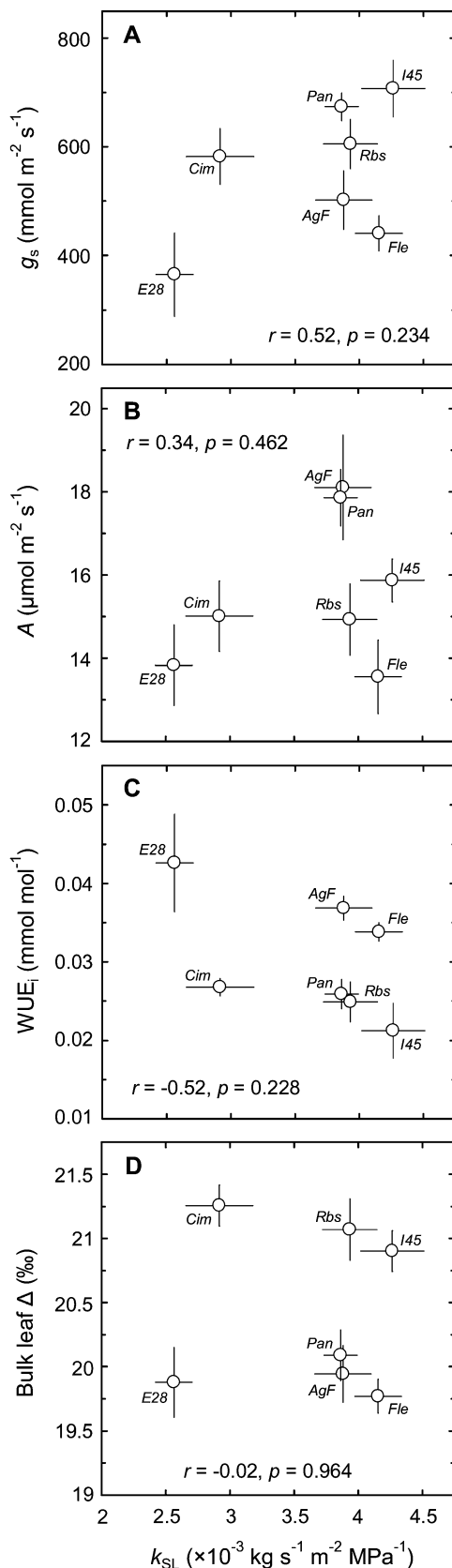


Fig. 6. Stomatal conductance [g_s , (A)], net CO_2 assimilation rate [A , (B)]; intrinsic water-use efficiency [WUE_i , (C)], and bulk leaf carbon isotope discrimination [Δ , (D)] as a function of leaf-specific hydraulic conductance (k_{SL}). Values are genotypic means \pm SE

which integrates diurnal gas exchange dynamics over the leaf ontogeny. The bulk of the literature points to a lack of consensus about the relationship between hydraulic efficiency and WUE, since positive (Sobrado, 2000, 2003; Drake and Franks, 2003; Kocacinar and Sage, 2003, 2004; Santiago *et al.*, 2004; Kocacinar *et al.*, 2008), negative (Pantek, 1996; Campanello *et al.*, 2008; Ducrey *et al.*, 2008; Martínez-Vilalta *et al.*, 2009), or no relationships (Preston and Ackerly, 2003; Edwards, 2006) may occur depending on the life history of the species or populations. Other issues that are likely to influence the direction and the strength of the relationship include (i) the way g_s can be related to hydraulic function (Ducrey *et al.*, 2008); (ii) how g_s and photosynthetic capacity are related to each other and to what extent each drives the variations in WUE under a particular environment; and (iii) the relative range of variation in WUE as compared with other features influencing xylem hydraulics such as variations in depth and architecture of roots, root to shoot allocation, and water storage (Preston and Ackerly, 2003; Bhaskar *et al.*, 2007; Sperry *et al.*, 2008).

No evidence was found of structural/functional coordination between hydraulic function and stomatal characters. However, the genotypic variations in stomatal density strongly concurred with the genotypic variations observed in g_s and thus in WUE estimates; that is, genotypes with fewer stomata per unit leaf area displayed higher g_s and lower WUE, thereby indicating the coupling of leaf water loss to stomatal characteristics. These results are in line with others including poplar (Dillen *et al.*, 2008; Sekiya and Yano 2008), but contrast greatly with the model of Nobel (1999) and with most experimental evidence from other studies (Pearce *et al.*, 2005; Xu and Zhou, 2008; Franks *et al.*, 2009), suggesting that high stomatal density allows the realization of high g_s . In fact, other stomatal characteristics such as pore depth, effective pore width, actual percentage of functional stomata, and potential trade-offs between these characteristics are also likely to influence g_s (Aasamaa *et al.*, 2001; Franks *et al.*, 2009) and should be considered in order to address the real significance of a negative relationship between g_s and stomatal density. Also perhaps the most interesting aspect of stomatal characters in the context of hydraulic coordination is the SPI as the SPI has proved to be a strong and predictive indicator of maximum leaf hydraulic conductance (k_{leaf}) across a broad range of species with contrasting ecological function (Sack *et al.*, 2003, 2005). Values of SPI recorded for the eight genotypes were in the range of others previously reported for temperate and tropical woody species (Sack *et al.*, 2003, 2005) and were strongly related to g_s and WUE estimates, suggesting a possible coordination between k_{leaf} and leaf water fluxes. However, as

(values for k_{SL} and k_{SS} represent genotypic means over 2007 and 2008). Regression lines are not shown as none of the regression was significant (Pearson's correlation coefficients, r). Genotype abbreviations are as in Fig. 1.

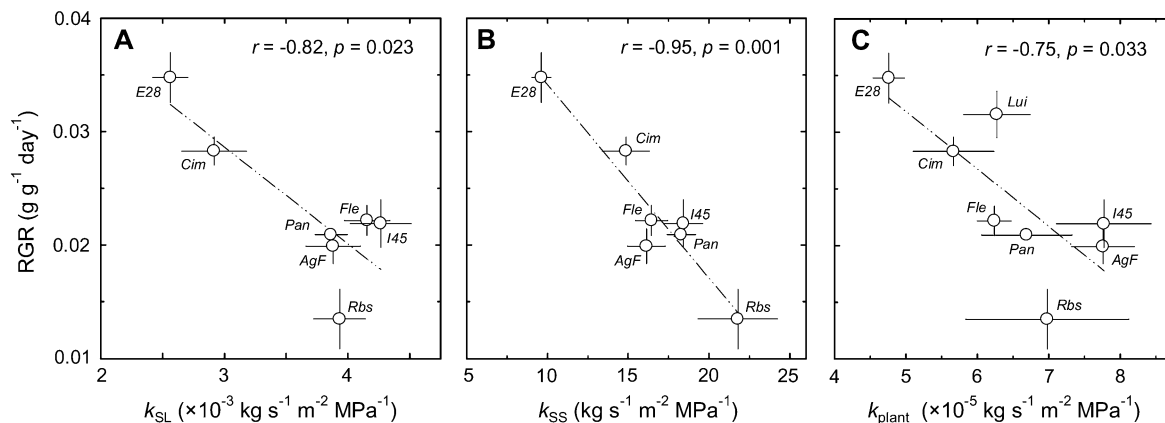


Fig. 7. The relative growth rate (RGR) as a function of (A) leaf-specific hydraulic conductance (k_{SL}), (B) xylem-specific hydraulic conductance (k_{SS}), and (C) apparent whole-plant leaf-specific hydraulic conductance (k_{plant}). Values are genotypic means \pm SE (values for k_{SL} and k_{SS} represent genotypic means over 2007 and 2008). The dash-dotted lines are linear regressions fitted to the data (Pearson's correlation coefficients, r). Genotype abbreviations are as in Fig. 1.

variations in SPI were mostly driven by stomatal density, this resulted in an apparently uncommon scenario of coordination, high SPI being coordinated with low g_s and thus high WUE.

Coordination of hydraulic architecture with whole-plant growth performance

Across genotypes, there was a strong negative scaling between estimates of water transport efficiency and RGR, indicating that hydraulic architecture and relative growth performance are intimately linked in poplar. However, this pattern contrasts with expectations from the Ohm's law analogue and other results indicating that net assimilation rates, height increment rates, and biomass production increase with increasing leaf-specific hydraulic efficiency across a broad range of tree species (Vander Willigen and Pammenter, 1998; Campanello *et al.*, 2008; Ducrey *et al.*, 2008). In addition, the cross-comparison of species with different life history types indicates that early successional colonizing species are characterized by greater hydraulic efficiency as compared with slow-growing later successional species (Tyree *et al.*, 1998; Pratt *et al.*, 2010). The fact that gas exchange rates were apparently uncoupled from growth performance, as already observed in poplar including *P. deltoides* \times *P. nigra* (Barigah *et al.*, 1994; Monclus *et al.*, 2006), would explain why k_{plant} and k_{SL} did not scale positively with RGR, but does not give the rationale for an opposite relationship. Alternatively, one may hypothesize that a large canopy area, which is the most important factor promoting biomass production in poplar species and related hybrids (Marron *et al.*, 2005; Monclus *et al.*, 2005; Marron and Ceulemans, 2006), would have resulted in a low k_{SL} (Comstock, 2000), thereby explaining the negative relationship, but this was not clearly apparent in the present data since most of the variations in k_{SL} originated from variations in k_{SS} rather than $A_X:A_L$. Actually, measurements of plant hydraulic conductance using the HPFM are representative of a fixed developmental stage, while growth efficiency as inferred

from RGR is driven by multiple components encompassing the leaf mass ratio (which reflects biomass partitioning to leaves), SLA (which reflects leaf morphology), and net assimilation rate (which reflects leaf function), each with a more or less predominant effect over the time dimension depending on environmental conditions (Shiple, 2000). Elucidating the functional basis of the relationship between hydraulics and growth performance will therefore necessitate a more comprehensive and temporal-integrated framework.

Somewhat unexpected was the positive relationship previously reported between xylem safety and growth potential (Fichot *et al.*, 2010), since increased xylem resistance to cavitation is often thought to be costly for plant growth (Wikberg and Ögren, 2004; Cochard *et al.*, 2007b). Actually, this pattern can be simply explained through the series of trade-offs occurring on the one hand between hydraulic efficiency and xylem safety and on the other hand between hydraulic efficiency and growth potential. Taken together, these results suggest that the supposed cost for increased safety was more than counterbalanced by the competitive advantage of displaying a lower hydraulic efficiency.

Conclusion

This study illustrated significant variations in hydraulic architecture among eight unrelated *P. deltoides* \times *P. nigra* genotypes. Hydraulic function appeared to be intimately linked to growth performance, while weakly, if at all, to WUE estimates. The strong but uncommon negative relationship linking hydraulic efficiency to RGR combined with the trade-off evidenced between hydraulic efficiency and xylem resistance to cavitation provided the rationale for the unexpected positive link previously observed between xylem resistance to cavitation and growth performance (Fichot *et al.*, 2010). More comprehensive work is now needed to disentangle the functional basis for low hydraulic efficiency to be associated with high growth potential, and

to investigate whether these relationships are specific to *P. deltooides* × *P. nigra* hybrids or can be extended to other *Populus* genetic backgrounds.

Acknowledgements

Isabelle Le Jan, Jean-Michel Petit, and Didier Delay at Orleans University, Marc Villar at INRA Orleans, and Bernard Clerc at INRA Nancy are thanked for their help during field experiments. We acknowledge Françoise Laurans for her help in the histological lab. We also acknowledge the logistic support provided by Ludovic Pasquier and Patrick Poursat at the INRA experimental station of Orleans during the field survey. Claude Brechet and Christian Hossann at the technical platform of Functional Ecology (INRA Nancy) are thanked for analysing $\delta^{13}\text{C}$ samples on the IRMS. Hardwood cuttings from the eight genotypes were kindly provided by Olivier Forestier from the State Forestry Nursery of Guéméné-Penfao (Loire Atlantique, France). RF, SC, and CD were Junior Researchers. RF was supported by a PhD grant from the 'French Ministry of Higher Education and Research'.

References

- Aasamaa K, Söber A, Rahi M.** 2001. Leaf anatomical characteristics associated with shoot hydraulic conductance, stomatal conductance and stomatal sensitivity to changes of leaf water status in temperate deciduous trees. *Australian Journal of Plant Physiology* **28**, 765–774.
- Alder NN, Pockman WT, Sperry JS, Nuismer S.** 1997. Use of centrifugal force in the study of xylem cavitation. *Journal of Experimental Botany* **48**, 665–674.
- Barigah TS, Saugier B, Mousseau M, Guittet J, Ceulemans R.** 1994. Photosynthesis, leaf area and productivity of 5 poplar clones during their establishment year. *Annals of Forest Science* **51**, 613–625.
- Becker P, Tyree MT, Tsuda M.** 1999. Hydraulic conductances of angiosperms versus conifers: similar transport sufficiency at the whole-plant level. *Tree Physiology* **19**, 445–452.
- Bhaskar R, Valiente-Banuet A, Ackerly DD.** 2007. Evolution of hydraulic traits in closely related species pairs from Mediterranean and non-Mediterranean environments of North America. *New Phytologist* **176**, 718–726.
- Brodribb TJ, Feild TS.** 2000. Stem hydraulic supply is linked to leaf photosynthetic capacity: evidence from New Caledonian and Tasmanian rainforests. *Plant, Cell and Environment* **23**, 1381–1388.
- Brodribb TJ, Feild TS, Jordan GJ.** 2007. Leaf maximum photosynthetic rate and venation are linked by hydraulics. *Plant Physiology* **144**, 1890–1898.
- Brodribb TJ, Holbrook NM, Gutiérrez MV.** 2002. Hydraulic and photosynthetic coordination in seasonally dry tropical forest trees. *Plant, Cell and Environment* **25**, 1435–1444.
- Brodribb TJ, Holbrook NM, Zwieniecki MA, Palma B.** 2005. Leaf hydraulic capacity in ferns, conifers and angiosperms: impacts on photosynthetic maxima. *New Phytologist* **165**, 839–846.
- Bucci SJ, Scholz FG, Goldstein G, Meinzer FC, Franco AC, Campanello PI, Villalobos-Vega R, Bustamante M, Miralles-Wilhelm F.** 2006. Nutrient availability constrains the hydraulic architecture and water relations of savannah trees. *Plant, Cell and Environment* **29**, 2153–2167.
- Campanello PI, Gatti MG, Goldstein G.** 2008. Coordination between water-transport efficiency and photosynthetic capacity in canopy tree species at different growth irradiances. *Tree Physiology* **28**, 85–94.
- Caquet B, Barigah TS, Cochard H, Montpied P, Collet C, Dreyer E, Epron D.** 2009. Hydraulic properties of naturally regenerated beech saplings respond to canopy opening. *Tree Physiology* **29**, 1395–1405.
- Cochard H, Casella E, Mencuccini M.** 2007b. Xylem vulnerability to cavitation varies among poplar and willow clones and correlates with yield. *Tree Physiology* **27**, 1761–1767.
- Cochard H, Coll L, Le Roux X, Ameglio T.** 2002. Unravelling the effects of plant hydraulics on stomatal closure during water stress in walnut. *Plant Physiology* **128**, 282–290.
- Cochard H, Damour G, Bodet C, Ibrahim T, Poirier M, Ameglio T.** 2005. Evaluation of a new centrifuge technique for rapid generation of xylem vulnerability curves. *Physiologia Plantarum* **124**, 410–418.
- Cochard H, Venisse JS, Barigah TS, Brunel N, Herbette S, Guillot A, Tyree MT, Sakr S.** 2007a. Putative role of aquaporins in variable hydraulic conductance of leaves in response to light. *Plant Physiology* **143**, 122–133.
- Comstock JP.** 2000. Variation in hydraulic architecture and gas-exchange in two desert sub-shrubs, *Hymenoclea salsola* (T. & G.) and *Ambrosia dumosa* (Payson). *Oecologia* **125**, 1–10.
- Dillen SY, Marron N, Koch B, Ceulemans R.** 2008. Genetic variation of stomatal traits and carbon isotope discrimination in two hybrid poplar families (*Populus deltooides* 'S9-2' × *P. nigra* 'Ghoy' and *P. deltooides* 'S9-2' × *P. trichocarpa* 'V24'). *Annals of Botany* **102**, 399–407.
- Dillen SY, Marron N, Sabatti M, Ceulemans R, Bastien C.** 2009. Relationships among productivity determinants in two hybrid poplar families grown during three years at two contrasting sites. *Tree Physiology* **29**, 975–987.
- Drake PL, Franks PJ.** 2003. Water resource partitioning, stem xylem hydraulic properties, and plant water use strategies in a seasonally dry riparian tropical rainforest. *Oecologia* **137**, 321–329.
- Ducrey M, Huc R, Ladjal M, Guehl JM.** 2008. Variability in growth, carbon isotope composition, leaf gas exchange and hydraulic traits in the eastern Mediterranean cedars *Cedrus libani* and *C. brevifolia*. *Tree Physiology* **28**, 689–701.
- Edwards EJ.** 2006. Correlated evolution of stem and leaf hydraulic traits in *Pereskia* (Cactaceae). *New Phytologist* **172**, 479–489.
- Farquhar GD, Ehleringer JR, Hubick KT.** 1989. Carbon isotope discrimination and photosynthesis. *Annual Review of Plant Physiology and Plant Molecular Biology* **40**, 503–537.
- Farquhar GD, O'Leary MH, Berry JA.** 1982. On the relationship between carbon isotope discrimination and the intercellular carbon dioxide concentration in leaves. *Australian Journal of Plant Physiology* **9**, 121–137.

- Fichot R, Barigah TS, Chamaillard S, Le Thiec D, Laurans F, Cochard H, Brignolas F.** 2010. Common trade-offs between xylem resistance to cavitation and other physiological traits do not hold among unrelated *Populus deltoides* × *Populus nigra* genotypes. *Plant, Cell and Environment* **33**, 1553–1568.
- Fichot R, Laurans F, Monclus R, Moreau A, Pilate G, Brignolas F.** 2009. Xylem anatomy correlates with gas exchange, water-use efficiency and growth performance under contrasting water regimes: evidence from *Populus deltoides* × *Populus nigra* hybrids. *Tree Physiology* **29**, 1537–1549.
- Franks PJ, Drake PL, Beerling DJ.** 2009. Plasticity in maximum stomatal conductance constrained by negative correlations between stomatal size and density: an analysis using *Eucalyptus globulus*. *Plant, Cell and Environment* **32**, 1737–1748.
- Hacke UG, Sperry JS, Pittermann J.** 2000. Drought experience and cavitation resistance in six shrubs from the great basin, Utah. *Basic Applied Ecology* **1**, 31–41.
- Heilman PE, Hinckley TM, Roberts DA, Ceulemans R.** 1996. Production physiology. In: Stettler RF, Bradshaw HD Jr, Heilman PE, Hinckley TM, eds. *Biology of Populus and its implications for management and conservation*. Ottawa, Ontario, Canada: NRC Research Press, 459–490.
- Hubbard RM, Ryan MG, Stiller V, Sperry JS.** 2001. Stomatal conductance and photosynthesis vary linearly with plant hydraulic conductance in ponderosa pine. *Plant, Cell and Environment* **24**, 113–121.
- Jacobsen AL, Pratt RB, Ewers FW, Davis SD.** 2007. Cavitation resistance among 26 chaparral species of southern California. *Ecological Monographs* **77**, 99–115.
- Kocacinar F, McKown AD, Sage TL, Sage RF.** 2008. Photosynthetic pathway influences xylem structure and function in *Flaveria*(Asteraceae). *Plant, Cell and Environment* **31**, 1363–1376.
- Kocacinar F, Sage RF.** 2003. Photosynthetic pathway alters xylem structure and hydraulic function in herbaceous plants. *Plant, Cell and Environment* **26**, 2015–2026.
- Kocacinar F, Sage RF.** 2004. Photosynthetic pathway alters hydraulic structure and function in woody plants. *Oecologia* **139**, 214–223.
- Maherali H, Moura CF, Caldeira MC, Willson CJ, Jackson RB.** 2006. Functional coordination between leaf gas exchange and vulnerability to xylem cavitation in temperate forest trees. *Plant, Cell and Environment* **29**, 571–583.
- Marron N, Ceulemans R.** 2006. Genetic variation of leaf traits related to productivity in a *Populus deltoides* × *Populus nigra* family. *Canadian Journal of Forest Research* **36**, 390–400.
- Marron N, Villar M, Dreyer E, Delay D, Boudouresque E, Petit JM, Delmotte FM, Guehl JM, Brignolas F.** 2005. Diversity of leaf traits related to productivity in 31 *Populus deltoides* × *Populus nigra* clones. *Tree Physiology* **25**, 425–435.
- Martínez-Vilalta J, Cochard H, Mencuccini M, et al.** 2009. Hydraulic adjustments of scots pine across Europe. *New Phytologist* **184**, 353–364.
- Martínez-Vilalta J, Prat E, Oliveras I, Piñol J.** 2002. Xylem hydraulic properties of roots and stems of nine Mediterranean woody species. *Oecologia* **133**, 19–29.
- McCulloh K, Sperry JS, Lachenbruch B, Meinzer FC, Reich PB, Voelker S.** 2010. Moving water well: comparing hydraulic efficiency in twigs and trunks of coniferous, ring-porous, and diffuse-porous saplings from temperate and boreal forests. *New Phytologist* **186**, 439–450.
- Meinzer FC.** 2002. Co-ordination of vapour and liquid phase water transport properties in plants. *Plant, Cell and Environment* **25**, 265–274.
- Meinzer FC, Grantz DA.** 1991. Coordination of stomatal, hydraulic, and canopy boundary layer properties: do stomata balance conductances by measuring transpiration? *Physiologia Plantarum* **83**, 324–329.
- Monclus R, Dreyer E, Delmotte FM, Villar M, Delay D, Boudouresque E, Petit JM, Marron N, Bréchet C, Brignolas F.** 2005. Productivity, leaf traits and carbon isotope discrimination in 29 *Populus deltoides* × *P. nigra* clones. *New Phytologist* **167**, 53–62.
- Monclus R, Dreyer E, Villar M, Delmotte FM, Delay D, Petit JM, Barbaroux C, Le Thiec D, Bréchet C, Brignolas F.** 2006. Impact of drought on productivity and water-use efficiency in 29 genotypes of *Populus deltoides* × *Populus nigra*. *New Phytologist* **169**, 765–777.
- Nardini A.** 2001. Are sclerophylls and mallacophylls hydraulically different? *Biologia Plantarum* **44**, 239–245.
- Nardini A, Salleo S.** 2000. Limitation of stomatal conductance by hydraulic traits: sensing or preventing xylem cavitation? *Trees* **15**, 14–24.
- Nardini A, Tyree MT.** 1999. Root and shoot hydraulic conductance of seven *Quercus* species. *Annals of Forest Science* **56**, 371–377.
- Nobel PS.** 1999. Resistances and conductances—transpiration. In: *Physicochemical and environmental plant physiology*, 2nd edn. San Diego: Academic Press, 301–303.
- Panek JA.** 1996. Correlations between stable carbon-isotope abundance and hydraulic conductivity in Douglas-fir across a climate gradient in Oregon, USA. *Tree Physiology* **16**, 747–755.
- Pataki DE, Oren R, Phillips N.** 1998. Responses of sap flux and stomatal conductance of *Pinus taeda* L. trees to stepwise reductions in leaf area. *Journal of Experimental Botany* **49**, 871–878.
- Pearce DW, Millard S, Bray DF, Rood SB.** 2005. Stomatal characteristics of riparian poplar species in a semi-arid environment. *Tree Physiology* **26**, 211–218.
- Pratt RB, Jacobsen AL, Ewers FW, Davis SD.** 2007. Relationships among xylem transport, biomechanics and storage in stems and roots of nine *Rhamnaceae* species of the California chaparral. *New Phytologist* **174**, 787–798.
- Pratt RB, North GB, Jacobsen AL, Ewers FE, Davis SD.** 2010. Xylem root and shoot hydraulics is linked to life history type in chaparral seedlings. *Functional Ecology* **24**, 70–81.
- Preston KA, Ackerly DD.** 2003. Hydraulic architecture and the evolution of shoot allometry in contrasting climates. *American Journal of Botany* **90**, 1502–1512.
- Sack L, Cowan PD, Jaikumar N, Holbrook NM.** 2003. The ‘hydrology’ of leaves: co-ordination of structure and function in temperate woody species. *Plant, Cell and Environment* **26**, 1343–1356.

- Sack L, Tyree MT, Holbrook NM.** 2005. Leaf hydraulic architecture correlates with regeneration irradiance in tropical rainforest trees. *New Phytologist* **167**, 403–413.
- Santiago LS, Goldstein G, Meinzer FC, Fisher JB, Machado K, Woodruff D, Jones T.** 2004. Leaf photosynthetic traits scale with hydraulic conductivity and wood density in Panamanian forest canopy trees. *Oecologia* **140**, 543–550.
- Sekiya N, Yano K.** 2008. Stomatal density of cowpea correlates with carbon isotope discrimination in different phosphorus, water and CO₂ environments. *New Phytologist* **179**, 799–807.
- Shiple B.** 2000. Plasticity in relative growth rate and its components following a change in irradiance. *Plant, Cell and Environment* **23**, 1207–1216.
- Sperry JS, Alder NN, Eastlack SE.** 1993. The effect of reduced hydraulic conductance on stomatal conductance and xylem cavitation. *Journal of Experimental Botany* **44**, 1075–1082.
- Sperry JS, Hacke UG, Oren R, Comstock JP.** 2002. Water deficits and hydraulic limits to leaf water supply. *Plant, Cell and Environment* **25**, 251–263.
- Sperry JS, Hacke UG, Wheeler JK.** 2005. Comparative analysis of end wall resistivity in xylem conduits. *Plant, Cell and Environment* **28**, 456–465.
- Sperry JS, Meinzer FC, McCulloh KA.** 2008. Safety and efficiency conflicts in hydraulic architecture: scaling from tissues to trees. *Plant, Cell and Environment* **31**, 632–645.
- Sobrado MA.** 2000. Relation of water transport to leaf gas exchange properties in three mangrove species. *Trees* **14**, 258–252.
- Sobrado MA.** 2003. Hydraulic characteristics and leaf water use efficiency in trees from tropical montane habitats. *Trees* **17**, 400–406.
- Tsuda M, Tyree MT.** 2000. Plant hydraulic conductance measured by the high pressure flow meter in crop plants. *Journal of Experimental Botany* **51**, 823–828.
- Tyree MT, Davis SD, Cochard H.** 1994. Biophysical perspectives of xylem evolution: is there a trade-off of hydraulic efficiency for vulnerability to dysfunction? *IAWA Journal* **15**, 335–360.
- Tyree MT, Ewers FW.** 1991. Tansley review no. 34. The hydraulic architecture of trees and other woody plants. *New Phytologist* **119**, 345–360.
- Tyree MT, Nardini A, Salleo S, Sack L, El Omari B.** 2005. The dependence of leaf hydraulic conductance on irradiance during HPPM measurements: any role for stomatal response? *Journal of Experimental Botany* **56**, 737–744.
- Tyree MT, Patiño S, Bennink J, Alexander J.** 1995. Dynamic measurements of root hydraulic conductance using a high-pressure flowmeter in the laboratory and field. *Journal of Experimental Botany* **46**, 83–94.
- Tyree MT, Velez V, Dalling JW.** 1998. Growth dynamics of root and shoot hydraulic conductance in seedlings of five neotropical tree species: scaling to show possible adaptation to differing light regimes. *Oecologia* **114**, 293–298.
- Tyree MT, Zimmermann MH.** 2002. *Xylem structure and the ascent of sap*, 2nd edn. Berlin: Springer-Verlag.
- Vander Willigen C, Pammenter NW.** 1998. Relationship between growth and xylem hydraulic characteristics of clones of *Eucalyptus* spp. at contrasting sites. *Tree Physiology* **18**, 595–600.
- Wheeler JK, Sperry JS, Hacke UG, Hoang N.** 2005. Inter-vessel pitting and cavitation in Rosaceae and other vesselled plants: a basis for a safety versus efficiency trade-off in xylem transport. *Plant, Cell and Environment* **28**, 800–812.
- Wikberg J, Ögren E.** 2004. Interrelationships between water use and growth traits in biomass-producing willows. *Trees* **18**, 70–76.
- Xu Z, Zhou G.** 2008. Responses of leaf stomatal density to water status and its relationship with photosynthesis in a grass. *Journal of Experimental Botany* **59**, 3317–3325.
- Yang S, Tyree MT.** 1994. Hydraulic architecture of *Acer saccharum* and *Acer rubrum*: comparisons of branches to whole trees and the contribution of leaves to hydraulic resistance. *Journal of Experimental Botany* **45**, 179–186.
- Zhang JL, Cao KF.** 2009. Stem hydraulics mediates leaf water status, carbon gain, nutrient-use efficiencies and plant growth rates across dipterocarp species. *Functional Ecology* **23**, 658–667.